

## Lipid Bilayers

International Edition: DOI: 10.1002/anie.201712017  
German Edition: DOI: 10.1002/ange.201712017

## Formation of pH-Resistant Monodispersed Polymer–Lipid Nanodiscs

Thirupathi Ravula<sup>+</sup>, Nathaniel Z. Hardin<sup>+</sup>, Sudheer Kumar Ramadugu, Sarah J. Cox, and Ayyalusamy Ramamoorthy\*

**Abstract:** Polymer lipid nanodiscs are an invaluable system for structural and functional studies of membrane proteins in their near-native environment. Despite the recent advances in the development and usage of polymer lipid nanodisc systems, lack of control over size and poor tolerance to pH and divalent metal ions are major limitations for further applications. A facile modification of a low-molecular-weight styrene maleic acid copolymer is demonstrated to form monodispersed lipid bilayer nanodiscs that show ultra-stability towards divalent metal ion concentration over a pH range of 2.5 to 10. The macro-nanodiscs (> 20 nm diameter) show magnetic alignment properties that can be exploited for high-resolution structural studies of membrane proteins and amyloid proteins using solid-state NMR techniques. The new polymer, SMA-QA, nanodisc is a robust membrane mimetic tool that offers significant advantages over currently reported nanodisc systems.

Controlled molecular self-assembly in the formation of soft nanomaterials has been a challenge in bio-nanotechnology.<sup>[1,2]</sup> Nanodiscs, lipid bilayers surrounded by an amphiphilic belt, are engineered soft nanomaterials that have been inspired from biological systems such as high-density lipo-particles (HDL).<sup>[3]</sup> These nanodiscs provide a lipid bilayer environment that is nearly like a native membrane, and they have been used to study the structure and function membrane proteins.<sup>[3–5]</sup> Recent developments have expanded the formation of nanodiscs using different types of amphiphilic systems such as proteins,<sup>[6–10]</sup> peptides,<sup>[11]</sup> and polymers.<sup>[12–15]</sup> Polymer nanodiscs exhibit significant advantages over conventional protein-based nanodiscs, such as detergent-free membrane protein extraction,<sup>[16]</sup> and they are devoid of interferences from the belt-forming protein or peptide.<sup>[17]</sup> Currently, no polymer nanodisc systems have been able to demonstrate precise control of size and morphology over a wide range of sizes or tolerance towards a broad range of pH and divalent metal ions.<sup>[16]</sup> These unique properties are needed to greatly expand the applicability of nanodisc technology. Herein we report the directed self-assembly of covalently modified

styrene maleic acid copolymer with lipid bilayers to form monodispersed nanodiscs that show ultra-stability towards a broad range of pH and divalent metal ion concentration. We also demonstrate the ability to control the size of the self-assembled nanodiscs and size-dependent unique magnetic alignment properties.

Synthesis of SMA-QA (styrene maleimide quaternary ammonium) was achieved by the treatment of a low-molecular-weight SMA (ca. 1.6 kDa) with (2-aminoethyl)trimethylammonium chloride hydrochloride in anhydrous dimethylformamide while heating in the presence of excess triethylamine. Maleimide formation was accomplished by a dehydration reaction using acetic anhydride, sodium acetate, and triethylamine (Figure 1 a). The newly synthesized SMA-QA polymer was characterized using FTIR spectroscopy and <sup>13</sup>CPMAS (cross-polarization magic-angle spinning) solid-state NMR experiments. FTIR spectrum of SMA-QA exhibits a shift in carbonyl C=O stretching frequency from 1774 cm<sup>-1</sup> to 1693 cm<sup>-1</sup>, showing the successful formation of maleimide (Supporting Information, Figure S1). The formation of SMA-QA was further confirmed by a <sup>13</sup>C CPMAS NMR spectrum (Figure 1 b): the peaks appearing at about 32 ppm and about 40 ppm are from the CH<sub>2</sub> group, and the peaks at about 53 ppm and about 62 ppm are from the methylene carbons associated with quaternary ammonium and methylene carbons, respectively. The observed change in the

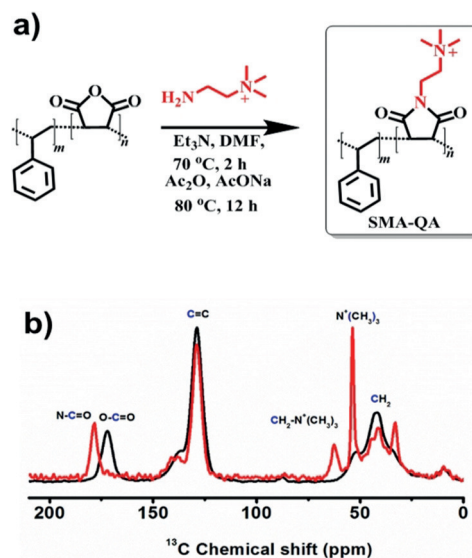


**Figure 1.** Synthesis and characterization of SMA-QA polymer. a) Modifications of SMA polymer to synthesize SMA-QA. b) <sup>13</sup>C CPMAS solid-state NMR spectra of SMA (black) and SMA-QA (red) polymers confirm the formation and successful completion of the chemical reaction. The SMA and SMA-QA polymers were further characterized using FTIR experiments (Supporting Information, Figure S1).

[\*] T. Ravula,<sup>[†]</sup> N. Z. Hardin,<sup>[†]</sup> S. K. Ramadugu, S. J. Cox, Prof. A. Ramamoorthy  
Biophysics Program and Department of Chemistry  
University of Michigan  
Ann Arbor, MI 48109-1055 (USA)  
E-mail: ramamoor@umich.edu

[†] These authors contributed equally to this work.

Supporting information (materials and methods, FTIR spectra of SMA-QA, orientation dependence of nitrogen-14 quadrupole coupling) and the ORCID identification number(s) for the author(s) of this article can be found under:  
<https://doi.org/10.1002/anie.201712017>.

chemical shift of the carbonyl carbon from about 172 (from the reactant SMA polymer) to about 178 ppm (from the product SMA-QA polymer) confirms the presence of malimide carbonyls and completion of the reaction and product formation (Figure 1b).

Next, we characterized the ability of SMA-QA to form lipid bilayer nanodiscs. Upon the addition of an aqueous solution of SMA-QA to a turbid solution of DMPC (1,2-dimyristoyl-sn-glycero-3-phosphocholine) multilamellar vesicles (MLVs), the turbid solution spontaneously became clear, indicating an efficient solubilization of MLVs by the polymer. The solubilization kinetics was followed by static light scattering (SLS) measurements. Figure 2b shows the SLS profiles of DMPC MLVs for different lipid to polymer weight ratios. As shown in Figure 2b, the large intense scattering observed for DMPC MLVs dramatically decreased upon the addition of SMA-QA polymer, demonstrating the solubilization of large DMPC MLVs into small size polymer-lipid nanodiscs. Our results further demonstrate that the kinetics of solubilization of MLVs by the polymer was found to depend on the ratio of DMPC:SMA-QA (Figure 2b). The rate of solubilization of MLVs was accelerated by the increase of the amount of SMA-QA.

The lipid nanodiscs formed by the SMA-QA polymer were subjected to size exclusion chromatography (SEC) to remove the free polymer. The SEC retention volume of purified nanodiscs was found to be dependent on the lipid:polymer ratio used in the nanodisc formation as shown in Figure 2c. The resulting nanodisc solutions were further characterized using dynamic light scattering (DLS) experi-

ments. The DLS profiles showed the presence of monodispersed nanodiscs of varying hydrodynamic radii (ca. 5 to ca. 13 nm) that were dependent on the ratio of DMPC to SMA-QA (Figure 2d). Then, the size and morphology of the resulting nanodiscs were characterized using transmission electron microscopy (TEM) images. The TEM images of DMPC:SMA-QA nanodiscs confirmed the presence of disc-shaped, monodispersed particles as shown in Figure 3. The expanded images shown in Figure 3 (bottom most row) show the size of individual nanodiscs and their remarkable circular shape.

The precise control over the size of nanodiscs for a wide range of sizes (ranging from 10 nm to 30 nm) inspired us to test their magnetic-alignment properties using solid-state NMR experiments under static conditions. The  $^{31}\text{P}$  (spin = 1/2) and  $^{14}\text{N}$  (spin = 1) spectra obtained from polymer nanodiscs are shown in Figure 4. The  $^{31}\text{P}$  NMR spectrum of DMPC:SMA-QA (1:0.25 w/w) shows a single narrow peak at about  $-16$  ppm (Figure 4a) demonstrating the magnetic alignment of polymer nanodiscs with the bilayer normal perpendicular to the magnetic field direction (Figure 4a).<sup>[14]</sup> Owing to the large size (ca. 30 nm diameter), the slow tumbling of nanodiscs (the large nanodiscs are also called macro-nanodiscs<sup>[14]</sup>) allows the magnetic alignment in an external magnetic field. On the other hand, a narrow peak was observed at the isotropic chemical shift frequency (ca.  $-2$  ppm) for small nanodiscs (ca. 10 nm), demonstrating their fast tumbling in the NMR timescale (Figure 4c).

The  $^{14}\text{N}$  NMR spectra of SMA-QA nanodiscs (ca. 30 nm) show three doublets corresponding to quadrupolar coupling values of about 14, 7.6, and 2.9 kHz (Figure 4b). The magnitude of the observed quadrupolar coupling is dependent on the orientation of the quaternary ammonium  $\text{C}^\beta\text{-N}$  bond vector with respect to the magnetic field direction (see the Supporting Information). The observed quadrupolar coupling magnitude of about 7.6 kHz arises from the choline group of DMPC and confirms the uniaxial orientation of nanodiscs with the lipid bilayer normal perpendicular to the magnetic field direction in agreement with  $^{31}\text{P}$  NMR data, as reported for other polymer nanodiscs.<sup>[18]</sup> The observed quadrupolar couplings of a magnitude of about 2.9 kHz and about 14 kHz are from the quaternary ammonium group of the SMA-QA polymer. The presence of these two distinct doublets suggests that SMA-QA polymer belt completely surrounds the lipid bilayer in

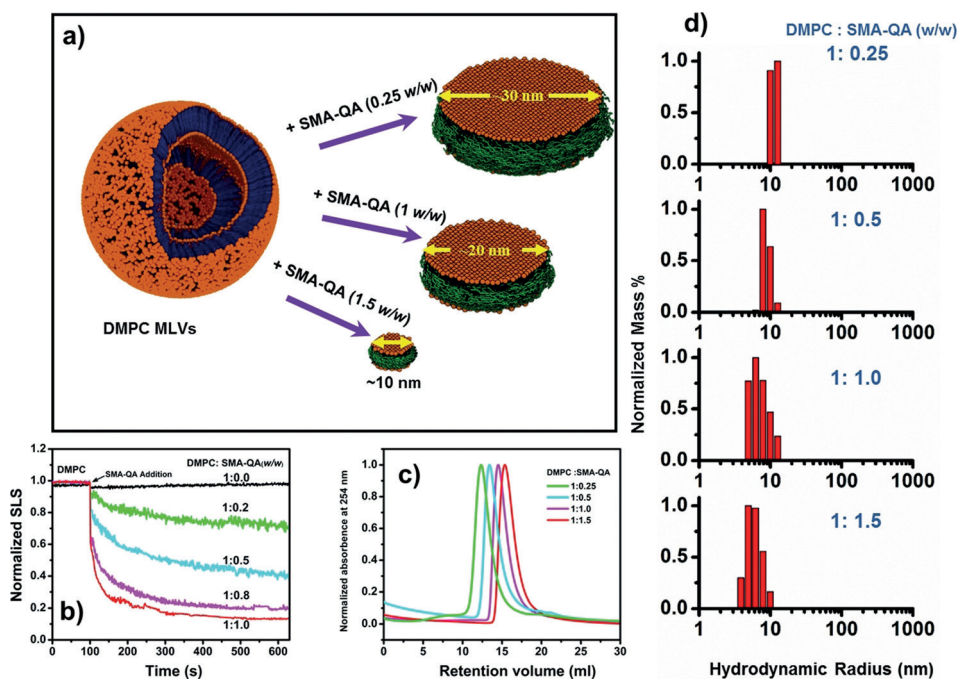


**Figure 2.** Formation and size tunability of SMA-QA lipid nanodiscs. a) The formation of SMA-QA nanodiscs of varying size. b) SLS profiles showing the kinetics of DMPC MLVs solubilization. c) Size exclusion profiles of nanodiscs made by varying the DMPC:SMA-QA weight ratio. d) DLS profiles of purified DMPC:SMA-QA nanodiscs demonstrate the formation of different size nanodiscs by varying the weight ratio of DMPC:SMA-QA.

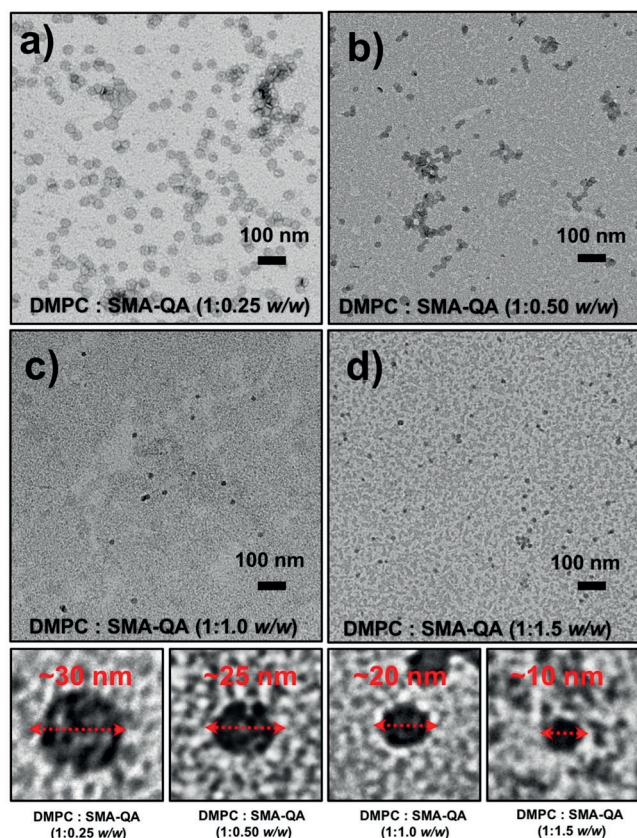


**Figure 3.** Remarkably monodispersed and circular shaped polymer nanodiscs revealed by TEM. a)–d) TEM images of DMPC:SMA-QA nanodiscs formed with the indicated lipid to polymer ratio. Expanded images of nanodiscs showing the remarkable disc shape of the nanodisc for different sizes (bottom most row).

a highly ordered fashion and with orientations as shown in Figure 4e, which is similar to the orientations of detergent molecules in aligned bicelles.<sup>[19]</sup> Additional experiments using paramagnetic lanthanide ions to tilt the orientation of lipid macro-nanodiscs would reveal the exact orientations of the polymer molecules. As expected, the  $^{14}\text{N}$  NMR spectrum of small nanodiscs (ca. 10 nm diameter) showed a single narrow peak at the isotropic chemical shift value (0 ppm) suggesting the fast tumbling nature of isotropic nanodiscs in agreement with  $^{31}\text{P}$  NMR data.

The major disadvantages of SMA and other polymers used to form nanodiscs is their poor stability towards pH and metal ions.<sup>[20]</sup> This instability is attributed to the presence of carboxylic/carboxylate groups that form the hydrophilic region of the amphiphilic polymer.<sup>[16]</sup> SMA-QA was specifically engineered and synthesized with a quaternary ammonium group as the hydrophilic portion of the polymer to increase the tolerance to pH and metal ions. The stability of the SMA-QA nanodiscs against pH and metal ion concentration was examined using SLS measurements (Figure 4 f,g). The SLS profiles of the DMPC:SMA-QA (1:1 w/w) nanodiscs showed no change in the scattering intensity over a wide range of pH (from about 2.5 to 10) and in the presence of metal ion concentrations up to 200 mM. These results signify the ultrahigh stability of DMPC:SMA-QA nanodiscs, further expanding the applicability of nanodisc technology to a wider range of biological and biomedical applications.

In conclusion, the newly developed SMA-QA polymer allows for the formation of monodispersed lipid nanodiscs with a precise size control and ultrahigh stability against pH (2.5–10) and metal ion concentrations up to 200 mM. The formation and stability of DMPC:SMA-QA nanodiscs were

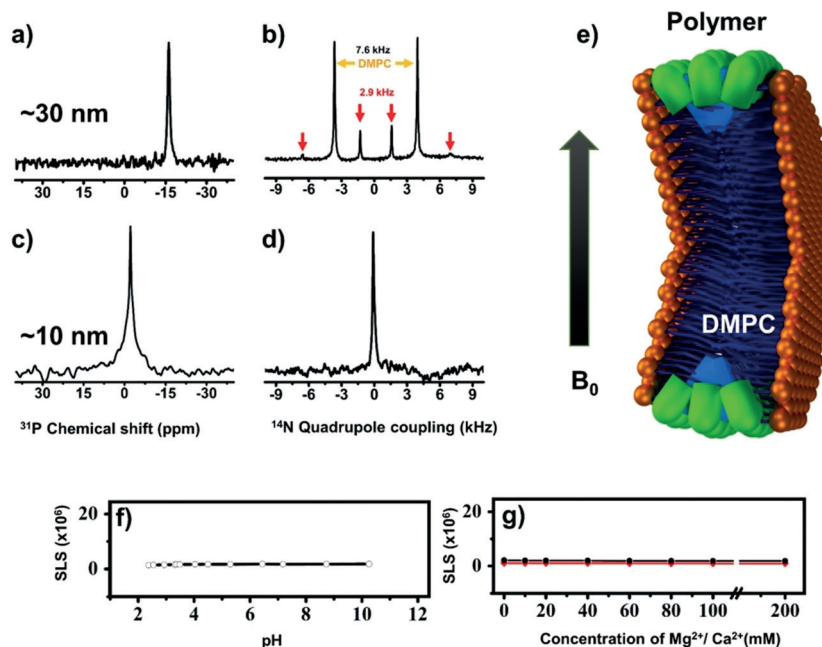


**Figure 4.** SMA-QA nanodiscs exhibit magnetic alignment and remarkable tolerance to pH and divalent metal ions. a)  $^{31}\text{P}$  and b)  $^{14}\text{N}$  NMR spectra of magnetically aligned large-size (ca. 30 nm diameter) nanodiscs made from DMPC:SMA-QA (1:0.25 w/w). c)  $^{31}\text{P}$  and d)  $^{14}\text{N}$  NMR spectra of isotropic nanodiscs (ca. 10 nm diameter) made from DMPC:SMA-QA (1:1.5 w/w). e) A nanodisc illustrating the orientations of the lipid headgroup and polymer in magnetically aligned nanodiscs. f),g) SLS profiles of DMPC:SMAQA (1:1 w/w) nanodiscs showing remarkable stability towards pH (f) and the presence of  $\text{Mg}^{2+}$  and  $\text{Ca}^{2+}$  (g) ions.

characterized using various biophysical experiments including solid-state NMR spectroscopy. The macro-nanodiscs (>20 nm diameter) showed magnetic alignment properties that can be utilized in the structural studies of membrane proteins by solid-state NMR techniques.<sup>[14,21–24]</sup> Because of these unique properties of SMA-QA polymer nanodiscs, SMA-QA is a robust membrane mimetic tool that offers significant advantages over all currently reported nanodisc systems, and therefore we foresee a significant expansion in the applicability of nanodisc technology. We expect direct and immediate impacts in the structural biology studies of those membrane proteins that are sensitive to pH and divalent metal ions<sup>[25–29]</sup> and amyloid proteins that self-assemble at the membrane interface.<sup>[30,31]</sup>

## Acknowledgements

This study was supported by the NIH (GM084018 to A.R.).

## Conflict of interest

The authors declare no conflict of interest.

**Keywords:** lipid bilayers · magnetic alignment · pH tolerance · polymer nanodiscs · styrene maleimide

**How to cite:** *Angew. Chem. Int. Ed.* **2018**, *57*, 1342–1345  
*Angew. Chem.* **2018**, *130*, 1356–1359

- [1] G. Whitesides, J. Mathias, C. Seto, *Science* **1991**, *254*, 1312–1319.  
[2] M. Sarikaya, C. Tamerler, A. K. Y. Jen, K. Schulten, F. Baneyx, *Nat. Mater.* **2003**, *2*, 577–585.  
[3] I. G. Denisov, S. G. Sligar, *Nat. Struct. Mol. Biol.* **2016**, *23*, 481–486.  
[4] I. G. Denisov, S. G. Sligar, *Chem. Rev.* **2017**, *117*, 4669–4713.  
[5] S. C. Lee, N. L. Pollock, *Biochem. Soc. Trans.* **2016**, *44*, 1011–1018.  
[6] T. H. Bayburt, Y. V. Grinkova, S. G. Sligar, *Nano Lett.* **2002**, *2*, 853–856.  
[7] M. L. Nasr, D. Baptista, M. Strauss, Z. J. Sun, S. Grigoriu, S. Huser, A. Pluckthun, F. Hagn, T. Walz, J. M. Hogle, G. Wagner, *Nat. Methods* **2017**, *14*, 49–52.  
[8] F. Hagn, M. Etzkorn, T. Raschle, G. Wagner, *J. Am. Chem. Soc.* **2013**, *135*, 1919–1925.  
[9] F. Hagn, G. Wagner, *J. Biomol. NMR* **2015**, *61*, 249–260.  
[10] T. H. Bayburt, S. G. Sligar, *FEBS Lett.* **2010**, *584*, 1721–1727.  
[11] M. Zhang, R. Huang, R. Ackermann, S. C. Im, L. Waskell, A. Schwendeman, A. Ramamoorthy, *Angew. Chem. Int. Ed.* **2016**, *55*, 4497–4499; *Angew. Chem.* **2016**, *128*, 4573–4575.  
[12] A. Oluwole, B. Danielczak, A. Meister, J. Babalola, C. Vargas, S. Keller, *Angew. Chem. Int. Ed.* **2017**, *56*, 1919–1924; *Angew. Chem.* **2017**, *129*, 1946–1951.  
[13] M. C. Orwick, P. J. Judge, J. Procek, L. Lindholm, A. Graziadei, A. Engel, G. Gröbner, A. Watts, *Angew. Chem. Int. Ed.* **2012**, *51*, 4653–4657; *Angew. Chem.* **2012**, *124*, 4731–4735.  
[14] T. Ravula, S. K. Ramadugu, G. Di Mauro, A. Ramamoorthy, *Angew. Chem. Int. Ed.* **2017**, *56*, 11466–11470; *Angew. Chem.* **2017**, *129*, 11624–11628.  
[15] I. D. Sahu, R. Zhang, M. M. Dunagan, A. F. Craig, G. A. Lorigan, *J. Phys. Chem. B* **2017**, *121*, 5312–5321.  
[16] S. C. Lee, T. J. Knowles, V. L. G. Postis, M. Jamshad, R. A. Parslow, Y.-p. Lin, A. Goldman, P. Sridhar, M. Overduin, S. P. Muench, T. R. Dafforn, *Nat. Protoc.* **2016**, *11*, 1149–1162.  
[17] J. M. Dörr, M. C. Koorengel, M. Schafer, A. V. Prokofyev, S. Scheidelaar, E. A. van der Crujisen, T. R. Dafforn, M. Balduis, J. A. Killian, *Proc. Natl. Acad. Sci. USA* **2014**, *111*, 18607–18612.  
[18] V. S. K. Ramadugu, G. M. Di Mauro, T. Ravula, A. Ramamoorthy, *Chem. Commun.* **2017**, *53*, 10824–10826.  
[19] S. V. Dvinskikh, K. Yamamoto, U. H. Durr, A. Ramamoorthy, *J. Magn. Reson.* **2007**, *184*, 228–235.  
[20] T. Ravula, N. Z. Hardin, S. K. Ramadugu, A. Ramamoorthy, *Langmuir* **2017**, *33*, 10655–10662.  
[21] S. H. Park, S. Berkamp, G. A. Cook, M. K. Chan, H. Viadiu, S. J. Opella, *Biochemistry* **2011**, *50*, 8983–8985.  
[22] U. H. Dürr, M. Gildenberg, A. Ramamoorthy, *Chem. Rev.* **2012**, *112*, 6054–6074.  
[23] H. Qin, Y. Miao, T. A. Cross, R. Fu, *J. Phys. Chem. B* **2017**, *121*, 4799–4809.  
[24] E. S. Salnikov, C. Aisenbrey, F. Aussenac, O. Ouari, H. Sarrouj, C. Reiter, P. Tordo, F. Engelke, B. Bechinger, *Sci. Rep.* **2016**, *6*, 20895.  
[25] V. Postis, S. Rawson, J. K. Mitchell, S. C. Lee, R. A. Parslow, T. R. Dafforn, S. A. Baldwin, S. P. Muench, *Biochim. Biophys. Acta Biomembr.* **2015**, *1848*, 496–501.  
[26] L. S. Brown, V. Ladizhansky, *Protein Sci.* **2015**, *24*, 1333–1346.  
[27] D. P. Staus, R. T. Strachan, A. Manglik, B. Pani, A. W. Khsai, T. H. Kim, L. M. Wingler, S. Ahn, A. Chatterjee, A. Masoudi, A. C. Kruse, E. Pardon, J. Steyaert, W. I. Weis, R. S. Prosser, B. K. Kobilka, T. Costa, R. J. Lefkowitz, *Nature* **2016**, *535*, 448–452.  
[28] Y. Gao, E. Cao, D. Julius, Y. Cheng, *Nature* **2016**, *534*, 347–351.  
[29] N. Das, D. T. Murray, T. A. Cross, *Nat. Protoc.* **2013**, *8*, 2256–2270.  
[30] D. C. Rodriguez Camargo, K. J. Korshavn, A. Jussupow, K. Raltchev, D. Goricanec, M. Fleisch, R. Sarkar, K. Xue, M. Aichler, G. Mettenleiter, A. K. Walch, C. Camilloni, F. Hagn, B. Reif, A. Ramamoorthy, *eLife* **2017**, *6*, e31226.  
[31] R. Ahmed, B. VanSchouwen, N. Jafari, X. Ni, J. Ortega, G. Melacini, *J. Am. Chem. Soc.* **2017**, *139*, 13720–13734.

Manuscript received: November 22, 2017

Accepted manuscript online: December 12, 2017

Version of record online: January 8, 2018